Geosciences and Engineering, Vol. 14, No. 1 (2026), pp. 85–109.
https://doi.org/10.33030/geosciences.2026.01.007

MINERALOGICAL INVESTIGATION OF Ni- AND Co-BEARING SULFIDES FROM THE FELSŐCSATÁR TALC SCHIST, HUNGARY

MÁTÉ ZS. LESKÓ[1]*, MONIKA FEICHTER[2], DÉLIA BULÁTKÓ-DEBUS[3], LÍVIA LESKÓNÉ MAJOROS[4], SÁNDOR SZAKÁLL[5]
[1,3,4,5] *Institute of Exploration Geosciences, University of Miskolc, Hungary*
[2] *Chair of Resource Mineralogy, Technical University of Leoben, Austria;*
[1*] mate.lesko@uni-miskolc.hu
[2] monika.feichter@unileoben.ac.at,
[3] delia.bulatko-debus@uni-miskolc.hu
[4] livia.leskone@uni-miskolc.hu
[5] sandor.szakal@uni-miskolc.hu
[1*] https://orcid.org/0000-0003-1948-2380

Abstract: Nickel and cobalt are critical raw materials essential for modern technologies and the energy transition. This study presents a detailed mineralogical investigation of the Ni–Co-bearing sulfides from the Felsőcsatár talc deposit, western Hungary. SEM–EDS and WDS analyses identified Ni-bearing pyrrhotite, Ni-rich pentlandite, violarite–siegenite and cobaltite–gersdorffite solid solution series, Ni-bearing pyrite, millerite, and ullmannite. The geological setting and mineralogical observations suggest that Ni and Co were originally derived from the ultramafic–mafic protolith, whereas hydrothermal and/or metamorphic processes are interpreted to have remobilized these elements and led to the formation of the Ni–Co-bearing mineralization. Subsequent supergene alteration resulted in the transformation of pentlandite into violarite.

Keywords: *Felsőcsatár, Talc schist, Ni-Co mineralization, SEM-EDS/WDS*

1. INTRODUCTION

Nickel (Ni) and cobalt (Co) are among the most important critical and strategic raw materials due to their essential role in modern technologies and the global transition toward clean energy. They are widely used in rechargeable lithium-ion batteries for electric vehicles and energy storage systems, where they improve energy density, performance, and battery lifetime. Nickel is also a key component of stainless steel and high-performance superalloys, providing excellent corrosion resistance and mechanical strength. Cobalt is indispensable in aerospace alloys, catalysts, permanent magnets, and various electronic applications. The rapidly increasing demand for electric vehicles and renewable energy technologies has significantly increased the global consumption of both elements. At the same time, their supply is challenged by the geographic concentration of mining and processing, creating potential risks for global supply chains. Consequently, both nickel and cobalt are classified as critical or strategic raw materials by several governments and international organizations, including the European Union (Grohol and Veeh, 2023). Developing new domestic resources, improving recycling technologies, and gaining a better understanding of ore-forming processes have therefore become important priorities for ensuring a secure and sustainable supply of these metals. Consequently, detailed mineralogical and geochemical investigations of Ni–Co occurrences are increasingly important for improving our understanding of the processes controlling the distribution and enrichment of critical metals. For this reason, investigating areas with known Ni and Co enrichment is of strategic importance to both Hungary and the European Union.

Several Ni–Co mineral occurrences are known within the Carpathian region, particularly in the Western Carpathians. The historically most significant example is the Dobšiná deposit in Slovakia, which is characterized by high-grade hydrothermal Ni–Co–Fe–As mineralization dominated by arsenides and sulfarsenides, including gersdorffite, rammelsbergite and skutterudite (Kiefer et al., 2017). Smaller Ni–Co occurrences are also known at Ľubietová-Kolba and Čierna Lehota, where gersdorffite and Ni–Co arsenides and sulfarsenides are associated with metamorphic rocks and hydrothermal mineralization (Majzlan et al., 2022). These occurrences demonstrate the diversity of Ni–Co mineralization within the Carpathian region and provide important regional analogues for the mineralogical investigation of the Felsőcsatár occurrence.

In the mid-20th century, active talc exploration began near Felsőcsatár in western Hungary. During the subsequent mining operations, chemical analyses revealed elevated concentrations of Ni and Co in some samples (Böjtösné Varrók, 1965). Although the talc mine was closed in the late 1980s, a few previous studies have reported the presence of Ni- and Co-bearing minerals from the Felsőcsatár deposit (Ditrói-Puskás et al., 1999). However, these studies did not focus specifically on the Ni–Co mineralization, and a detailed mineralogical investigation of the Ni- and Co-bearing phases has not yet been conducted. Therefore, this study aims to identify the Ni- and Co-bearing mineral phases occurring in the talc schist from Felsőcsatár, Hungary.

2. Geological setting

The Kőszeg Mountains and Vashegy belong to the Alpine Penninic crystalline rocks and represent their easternmost occurrence (P on Figure 1). These rocks emerge from beneath the Austroalpine nappes as tectonic windows: the Kőszeg Mountains are part of the Rechnitz Window, whereas Vashegy forms an independent tectonic window (Pahr, 1980; Koller, 1985; Ratschbacher et al., 1990).

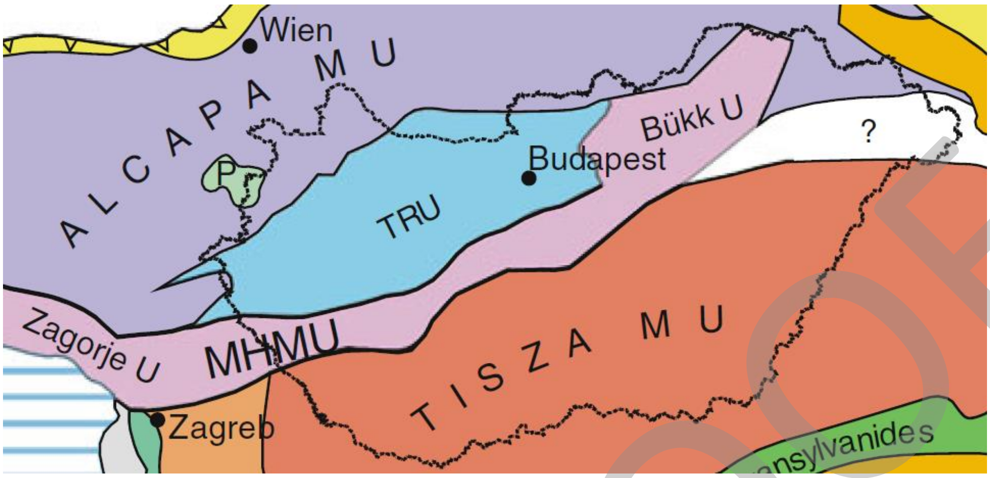

Figure 1

The main structural units of the pre-Cenozoic basement of Hungary. P: Penninic Unit; TRU: Transdanubian Range; MHMU: Mid-Hungarian Mega Unit (after Haas et al., 2010)

According to the classification by Koller (1980), the Rechnitz Series is composed of two major complexes: (1) an ophiolitic assemblage consisting of serpentinized ultramafic rocks, metagabbros, greenschists, and blueschists; and (2) a metasedimentary complex including calcareous phyllites, quartz phyllites, and coarse-grained metaconglomerate layers.

Both complexes underwent very low- to low-grade Alpine metamorphism involving three principal metamorphic phases (Koller, 1985; Frank et al., 1987; Demény and Dunkl, 1991). The earliest (Eoalpine) phase was limited to the ophiolitic rocks and is characterized by low-pressure, high-temperature ocean-floor metamorphism and metasomatism (P ≈ 1 kbar; T ≈ 400–750 °C).

The second phase represents the initial manifestation of Alpine metamorphism and affected both the ophiolites and part of the metasedimentary succession under low-temperature, high-pressure conditions. This event is associated with Cretaceous (~65 Ma) pumpellyite–actinolite facies metamorphism, estimated at pressures of 6–8 kbar and temperatures of 340–430 °C.

The third and youngest metamorphic phase produced low-temperature, low-pressure greenschist facies metamorphism (P ≈ 3 kbar; T ≈ 390–430 °C) across all lithologies. Zircon fission-track dating indicates metamorphic ages between 15 and 18.5 Ma. These ages are consistent with data reported from other parts of the Penninic domain. The oldest post-metamorphic cover sequence is of Late Miocene (Sarmatian) age.

3. Materials and Methods

The investigated area is located in western Hungary, near the Austrian border (Figure 2a). In the mid-20th century, systematic exploration for talc deposits began in the area. Approximately 80 exploration drill holes were drilled (Figure 2b–c), and underground mining commenced in the late 1950s. Mining operations continued until the late 1980s (Figure 2d–e).

Unfortunately, only samples of seven of the original drills are currently available, and their preservation is generally poor. Core samples were selected using the archived drill core catalogue; however, none of the sampled intervals contained Ni- or Co-bearing mineral phases. Therefore, the results presented in this paper are based on talc schist samples collected from the waste dump of the former talc mine. The examined samples are in the Herman Ottó Museum collection, Miskolc, Hungary.

Electron microprobe analyses (EMPA) of the Ni-Co-bearing sulphide minerals were performed by energy-dispersive (EDS) and wavelength-dispersive X-ray spectrometry (WDS). The element maps and the energy-dispersive X-ray spectroscopy measurements were carried out with a ThermoFisher Helios PFIB G4 CXe scanning electron microscope, with acceleration voltage ranging from 5–20 kV and beam current ranging from 0.4 nA–13 nA in the 3D Laboratory of the University of Miskolc.

The wavelength-dispersive X-ray spectrometry measurements were taken at the Technical University of Leoben using a JEOL JXA 8200 WD/ED Combined Microanalyzer. The acceleration voltage was 20 kV, and the beam current was 10 nA during the measurement. Other measurement parameters are given in Table 1. The following natural mineral standards were applied: millerite for Ni and S; skutterudite for Co and As and pyrite for Fe.

According to accepted international practice, WDS analyses were considered acceptable and included in this study only when the analytical total ranged between 99.0 and 101.0 wt%. The only exception was made for minerals of the violarite–siegenite solid solution series, for which analyses with totals between 98.5 and 101.0 wt% were also accepted. This slightly wider acceptance range was adopted because the violarite–siegenite aggregates commonly exhibit microporosity. Consequently, the analyzed volume may include microscopic voids, resulting in slightly lower analytical totals.

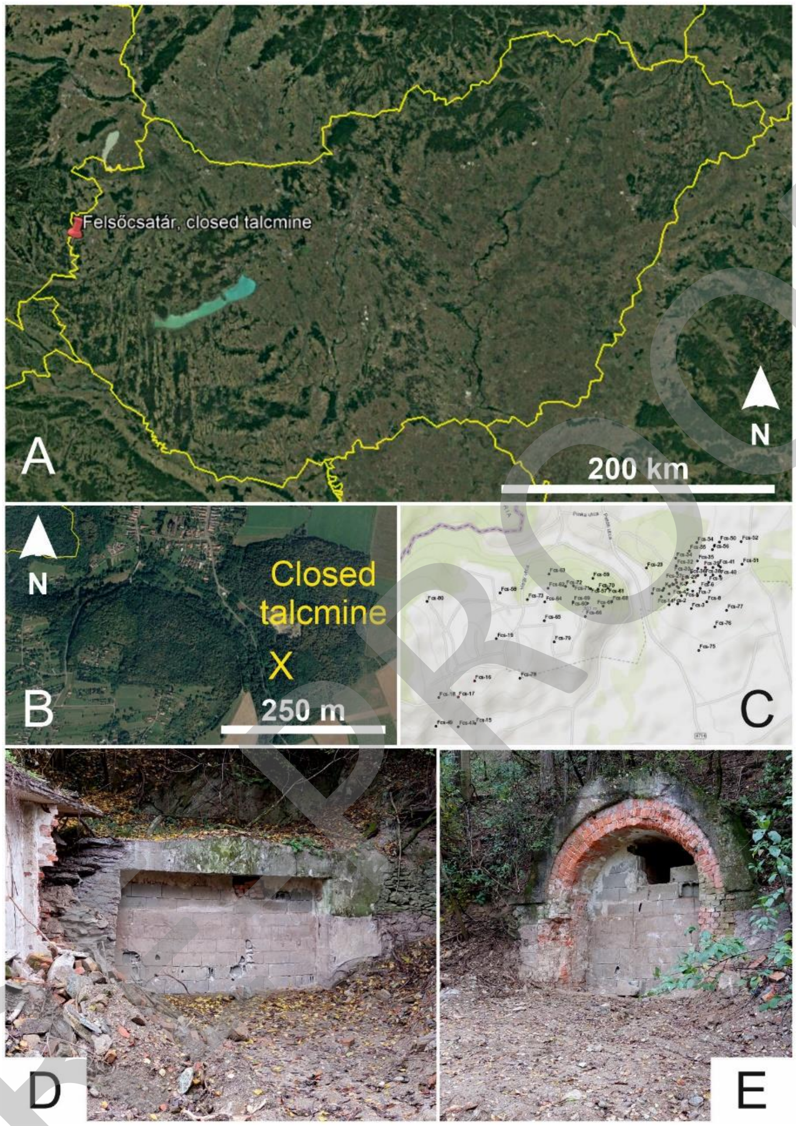

Figure 2
A and B: Location of Felsőcsatár (image: Google Earth); C: Location of the exploration drill holes (image: The Supervisory Authority for Regulatory Affairs, https://map.hugeo.hu/furas); D and E: the closed talc mine entrances at Felsőcsatár

Table 1

Measurement parameters of the WDS analyses

Measured element	S	Ni	Co	Fe	As
Analyzing crystal	PETJ	LIFH	LIFH	LIFH	TAP
Peak time (s)	20	20	20	20	20
Background time (s)	10/10	10/10	10/10	10/10	10/10
Background position (mm)	± 5	± 5	± 5	± 5	± 5

4. RESULTS

Our investigation identified seven different Ni- and Co-bearing phases and native gold in the studied samples. Phase identification was carried out using scanning electron microscopy coupled with energy-dispersive spectroscopy (SEM–EDS) and wavelength-dispersive spectroscopy (WDS). The identified Ni- and Co-bearing phases, together with their ideal chemical formulas, are listed below in decreasing order of abundance:

- Ni- and Co-bearing pyrrhotite, $Fe_{1-x}S$
- Ni rich pentlandite, $(Fe^{2+},Ni)_9S_8$
- Fe rich solid solution of violarite ($Fe^{2+}Ni^{3+}{}_2S_4$) – siegenite ($CoNi_2S_4$)
- Co-rich solid solution of cobaltite (CoAsS) – gersdorffite (NiAsS)
- Ni-bearing pyrite, FeS_2 (non official mineral as bravoite [1])
- Millerite, NiS
- Ullmannite, NiSbS

Greigite ($Fe^{2+}Fe^{3+}{}_2S_4$) was tentatively identified earlier, however, the WDS analyses performed in the present study did not confirm its presence.

Pyrrhotite

Pyrrhotite commonly occurs as grains a few hundred micrometers in size and is frequently associated with pentlandite (Figure 3). All analyzed pyrrhotite grains contain measurable amounts of both Ni and Co. The complete WDS analytical data are provided in Appendix Ia–c. The Fe–Ni–Co compositional variations of the analyzed pyrrhotite grains are illustrated in the ternary diagram shown in Figure 4, where the atomic proportions were calculated from WDS analyses and normalized to Fe + Ni + Co = 100 at.%. Summary statistics, including the minimum, maximum, mean, and median compositions, are presented in Table 2.

[1] *not an official mineral accepted by the International Mineralogical Association*

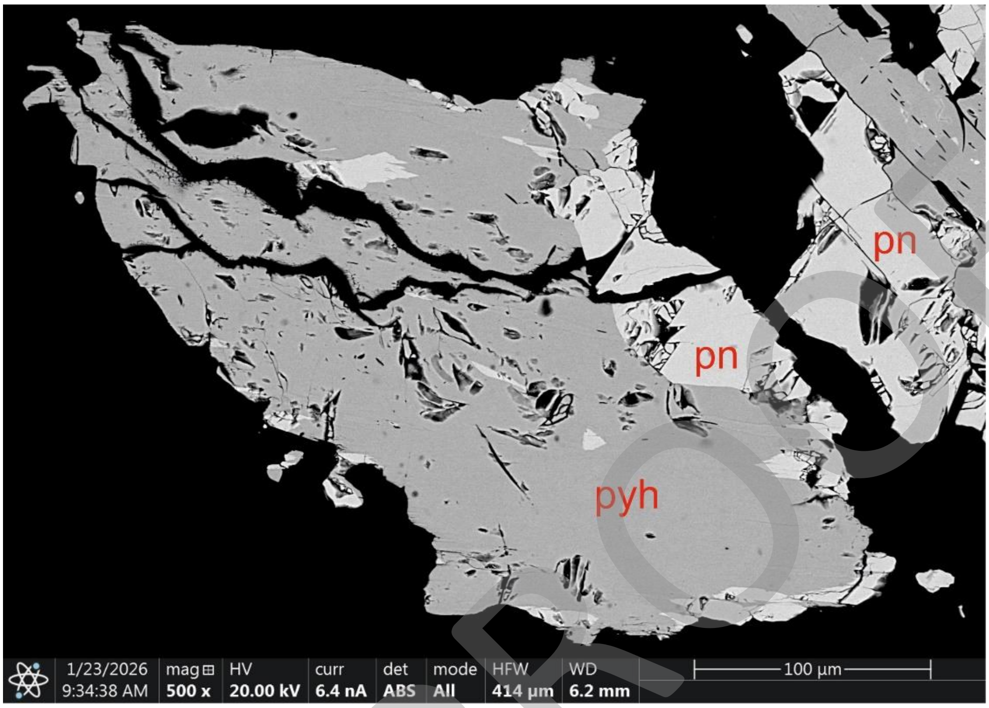

Figure 3

Representative *back-scattered electron (BSE) image* of pyrrhotite (pyh) and pentlandite (pn)

Table 2

The minimum, maximum, average and median values of 61 point analyses of pyrrhotite. Atomic proportions were calculated from WDS analyses and normalized to Fe + Ni + Co = 100 at.%

	Fe	Co	Ni
Minimum	87.46	0.22	5.01
Maximum	94.66	0.41	12.23
Average	90.95	0.30	8.75
Median	90.84	0.31	8.81

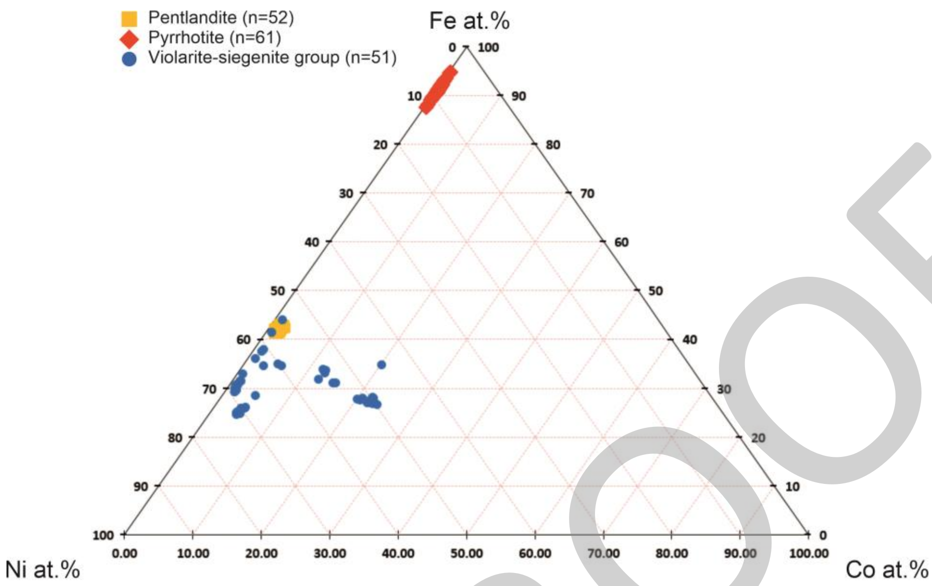

Figure 4

Fe–Ni–Co ternary diagram showing the atomic proportions of pyrrhotite, pentlandite, and violarite–siegenite-group minerals determined by WDS analyses. Atomic proportions were calculated from WDS weight percentages and normalized to Fe + Ni + Co = 100 at.%.

Pentlandite

Pentlandite occurs as anhedral to subhedral grains ranging from a few tens of micrometers to approximately 250 µm in size. It is most commonly associated with pyrrhotite and, less frequently, with violarite (Figure 3). Representative WDS analyses of pentlandite are listed in Appendix IIa–b. The Fe–Ni–Co compositional data are plotted in the ternary diagram shown in Figure 4, using atomic proportions calculated from WDS analyses and normalized to Fe + Ni + Co = 100 at.%. Most analyses cluster within a relatively narrow compositional range, indicating only limited chemical variability among the analyzed pentlandite grains. The corresponding minimum, maximum, mean, and median values are summarized in Table 3.

Table 3

The minimum, maximum, average and median values of 52 point analyses of pentlandite. Atomic proportions were calculated from WDS analyses and normalized to Fe + Ni + Co = 100 at.%

	Fe	**Co**	**Ni**
Minimum	41.17	0.94	55.12
Maximum	43.00	2.26	57.44
Average	41.83	1.65	56.52
Median	41.77	1.80	56.61

Violarite-siegenite group

Violarite occurs as grains ranging from a few tens of micrometers to approximately 250 µm in size. The analyzed grains form a compositional continuum within the violarite–siegenite solid solution series. The ideal chemical formula of violarite is $Fe^{2+}Ni^{3+}{}_2S_4$, whereas siegenite has the ideal formula $CoNi_2S_4$. All analyzed grains contain measurable amounts of Co, indicating partial substitution of Fe by Co. Representative SEM-EDS element maps reveal pronounced chemical inhomogeneity within individual grains (Figure 5). Co-enriched zones are common; however, none of the analyzed compositions reached the ideal siegenite end-member. Instead, some of their compositions lie close to the violarite–siegenite compositional boundary. The Fe–Ni–Co compositional variations are illustrated in the ternary diagram shown in Figure 4, where the atomic proportions were calculated from WDS analyses and normalized to Fe + Ni + Co = 100 at.%. Compared to pyrrhotite and pentlandite, the violarite–siegenite group minerals exhibit a considerably wider compositional range. The complete WDS analytical data are provided in Appendix IIIa–b.

Cobaltite–gersdorffite group

Cobaltite–gersdorffite group minerals occur as grains ranging from a few tens of micrometers to approximately 150 µm in size. Only two grains suitable for quantitative WDS analysis were identified. Both analyses correspond to Fe-bearing, Ni-rich cobaltite compositions within the cobaltite–gersdorffite solid solution series. Representative EDS elemental maps (Figure 5–6) reveal chemical zoning characterized by variations in the Co and Ni contents within individual grains. The complete WDS analytical data together with the calculated structural formulas are presented in Table 4.

Table 4

WDS analyses data of cobaltite-gersdorffite group minerals

As (wt%)	**S (wt%)**	**Fe (wt%)**	**Co (wt%)**	**Ni (wt%)**	**Calculated formula**
43.7	19.584	5.289	15.839	14.887	(Co0.45Ni0.42Fe0.16)As0.98S1.02
43.692	19.62	5.193	16.92	13.597	(Co0.48Ni0.39Fe0.16)As0.98S1.02

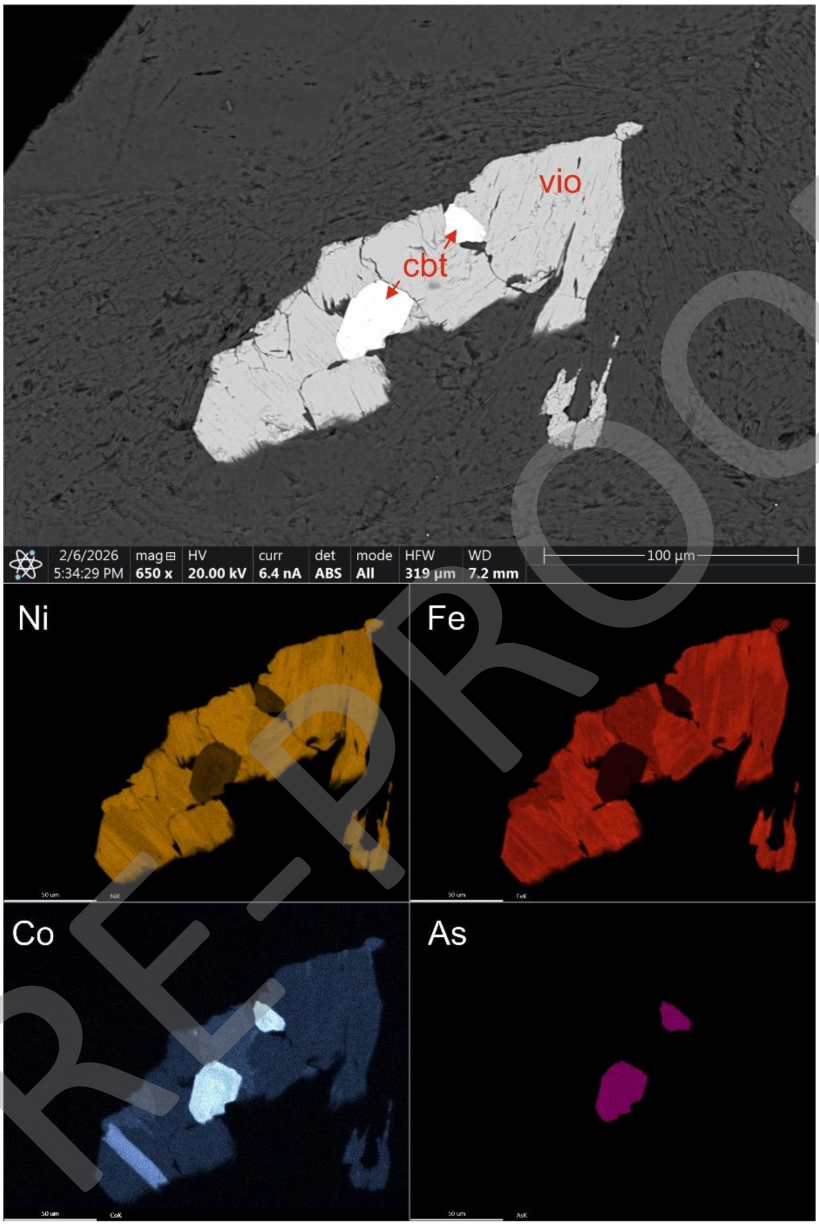

Figure 5

Upper panel: Back-scattered electron (BSE) image of violarite (vio) and cobaltite (cbt). Lower panels: SEM-EDS element map shows inhomogeneity of violarite (violarite–siegenite solid solution) and cobaltite (cobaltite–gersdorffite solid solution)

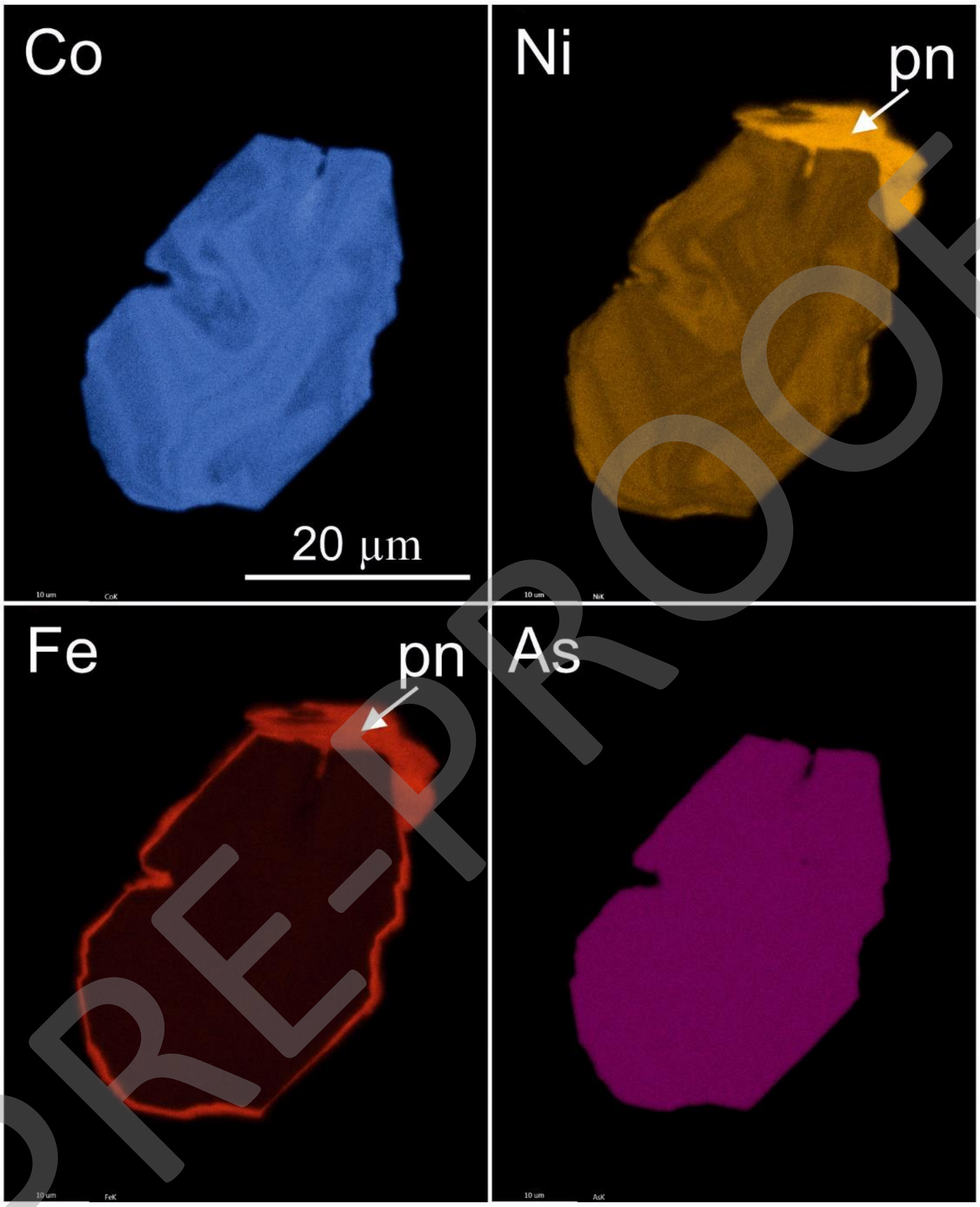

Figure 6

SEM-EDS element map of Fe-bearing cobaltite–gersdorffite solid solution and pentlandite (pn). Cobalt (blue) and nickel (yellow) show compositional zoning

Other Ni/Co phases

Several 1–2 µm Ni-bearing pyrite octahedra were observed in several areas (Figure 7). The grains were to small to WDS measurements. Only SEM-EDS results listed in Table 5.

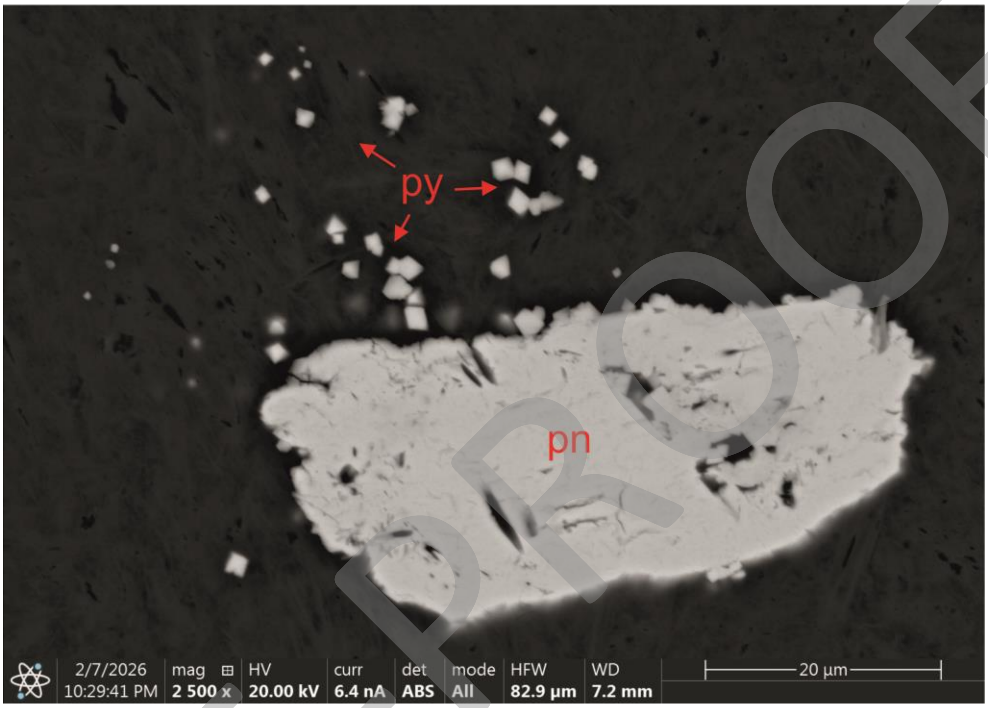

Figure 7

Back-scattered electron (BSE) image of 1-2 µm Ni-bearing pyrites (py) with pentlandite (pn)

Table 5

EDS analysis data of Ni-bearing pyrites

Fe (at.%)	Co (at.%)	Ni (at.%)	S (at.%)
19.6	0.9	12.6	66.8
20.6	0.5	11.8	67.1

Millerite was tentatively identified in a small grain adjacent to pyrrhotite; however, the quantitative analyses were affected by overlap with the neighboring pyrrhotite (Figure 8).

One grain of ullmannite was found next to a pentlandite (Figure 9).

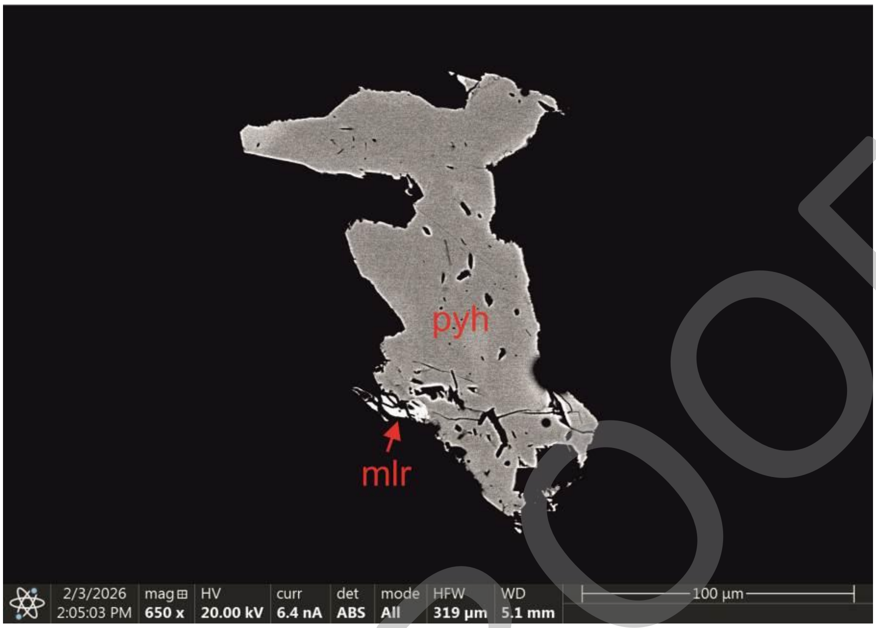

Figure 8

Back-scattered electron (BSE) image of a pyrrhotite grain (pyh) containing a small millerite grain (mlr) along its margin

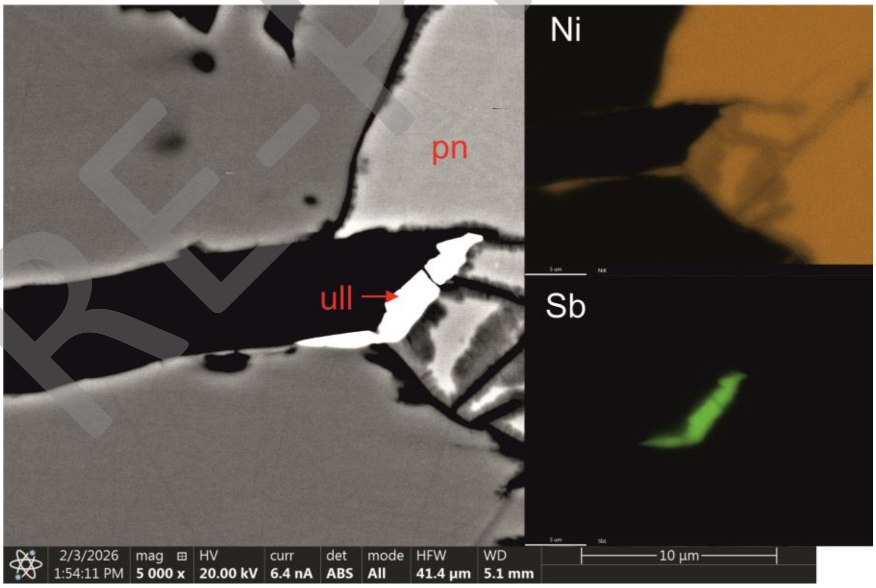

Figure 9

Back-scattered electron (BSE) image of a ullmannite (ull) at the margin of a pentlandite grain (pn) (left panel). SEM-EDS element map of Ni (yellow) and Sb (green)

Furthermore, in two samples native gold grains were found: 5 pieces in all 2–3 µm in size (Figure 11).

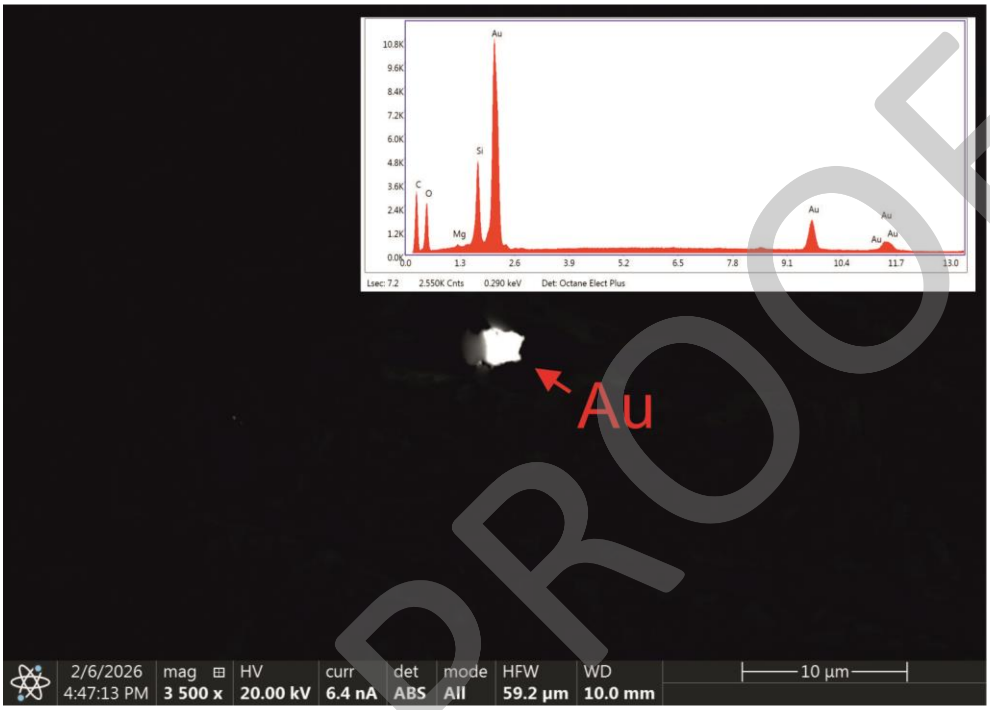

Figure 10
Representative back-scattered electron (BSE) image and EDS spectra of a native gold grain in the talc schist

5. Discussion and Conclusions

Nickel and cobalt deposits are commonly classified into three major genetic groups: magmatic, structure-related, and sedimentary deposits, each of which comprises several subtypes (Dill, 2010). The geological setting of the Felsőcsatár talc deposit differs markedly from that of typical sedimentary Ni–Co deposits; therefore, a sedimentary origin of the mineralization can be excluded. According to Dill (2010), sedimentary Ni deposits are mainly represented by lateritic Ni–Co deposits, shale-hosted polymetallic mineralization, and nickeliferous manganese nodules. Lateritic deposits typically develop through intense tropical to subtropical weathering of ultramafic rocks and are characterized by Ni enrichment in limonitic, saprolitic, and hydrosilicate-rich weathering profiles, whereas shale-hosted deposits are associated with organic-rich sedimentary successions. None of these characteristic geological settings or ore types is observed at Felsőcsatár. Nevertheless, supergene alteration processes likely played an important role in the formation of several of the identified

Ni- and Co-bearing secondary minerals. Likewise, a structure-related origin is considered unlikely, as these deposits are typically characterized by vein- or breccia-hosted mineralization (Dill, 2010), which is not observed at Felsőcsatár. The absence of vein-hosted mineralization and the close association of the sulfides with talc schist also argue against a typical hydrothermal vein-type deposit.

The origin of the Ni and Co mineralization is most likely associated with ultramafic/mafic protoliths, followed by remobilization of these elements during metamorphism. The two most abundant Ni- and Co-bearing minerals, pyrrhotite and pentlandite, exhibit relatively uniform chemical compositions, suggesting that they formed during one mineralizing event.

Compared with other Ni–Co mineral occurrences in the Carpathian region, the Felsőcsatár mineralization shows both similarities and important mineralogical differences. The historically significant Dobšiná deposit is characterized by hydrothermal Ni–Co–Fe–As veins dominated by arsenides and sulfarsenides, including gersdorffite, rammelsbergite and skutterudite (Kiefer et al., 2017). Similarly, the Ni–Co mineralization at Ľubietová-Kolba and Čierna Lehota consists predominantly of arsenides and sulfarsenides; gersdorffite is the dominant Ni–Co–Fe sulfarsenide at Ľubietová-Kolba, whereas skutterudite and pararammelsbergite are characteristic of Čierna Lehota (Majzlan et al., 2022). In contrast, the Felsőcsatár assemblage is dominated by Ni-bearing sulfides, particularly pyrrhotite, pentlandite and violarite–siegenite group minerals, while cobaltite–gersdorffite group minerals occur only as subordinate phases. Nevertheless, the occurrence of cobaltite–gersdorffite at Felsőcsatár provides a mineralogical link to the Western Carpathian Ni–Co occurrences. These similarities, together with the association of the Felsőcsatár mineralization with metamorphosed mafic–ultramafic rocks, are consistent with remobilization of Ni and Co during later hydrothermal and/or metamorphic processes, although the resulting mineral assemblage differs markedly from the As-rich hydrothermal systems of the Western Carpathians.

Violarite–siegenite group minerals are most commonly interpreted as supergene alteration products of pentlandite (Butt and Nickel, 1981). However, previous studies have also demonstrated that violarite may form during hydrothermal alteration (Tenailleau et al., 2006) or remain stable under hypogene conditions along the violarite–pentlandite tie line (Grguric, 2002). Based on the observed mineral assemblage and textural relationships, the violarite–siegenite group minerals identified in the Felsőcsatár talc schist most likely formed during supergene alteration of primary pentlandite. The violarite–siegenite phases occur in close association with pentlandite and show irregular replacement textures, locally developed along grain margins and fractures. No regularly oriented, lath- or flame-like violarite lamellae characteristic of hypogene exsolution from pentlandite (Grguric, 2002) were observed. These textures are therefore more consistent with the replacement of pentlandite than with an exsolution origin. The occurrence of Ni-bearing pyrite in the same mineral assemblage further supports secondary alteration of the primary Ni-bearing sulfides. Nevertheless, the available samples do not allow determination of whether this transformation occurred in situ within the original ore body during near-surface weathering or developed after mining while the material was exposed in the waste dump. Both scenarios remain possible.

The cobaltite–gersdorffite group minerals are mostly associated with pentlandite and were observed exclusively as inclusions within, or in direct contact with, pentlandite grains suggesting crystallization from the same primary sulfide assemblage. This close textural relationship suggests that both mineral phases are genetically related and most likely formed during the same mineralizing event.

The occurrence of Ni-bearing pyrite (bravoite) is consistent with the supergene alteration of primary Ni-bearing sulfides, as previously described by Dill (2010).

Because all investigated samples were collected from the waste dump of the abandoned talc mine, it was not possible to assign the results to their original spatial positions within the ore body. Consequently, no conclusions can be drawn regarding the spatial distribution of the Ni- and Co-bearing mineralization, and a reliable mineral resource estimation cannot be performed based on the available material. Accurate assessment of the spatial distribution and resource potential would require in situ sampling and additional investigations.

In conclusion, a detailed mineralogical investigation was carried out on the Ni- and Co-bearing mineralization of the talc schist at Felsőcsatár, western Hungary. The study identified Ni-bearing pyrrhotite (5–12 wt% Ni), Ni-rich pentlandite, violarite–siegenite solid solution series, cobaltite–gersdorffite solid solution series, millerite, and Ni-bearing pyrite (bravoite). The results demonstrate that the Ni and Co are hosted by several distinct sulfide phases, with the violarite–siegenite and cobaltite–gersdorffite solid solution series reflecting significant compositional variability. These findings provide the first comprehensive mineralogical characterization of the Ni–Co sulfide assemblage in the Felsőcsatár talc deposit and establish a basis for future investigations and exploration of the origin and economic significance of the mineralization.

Acknowledgments

„Supported by the University Research Scholarship Program of the Ministry for Culture and Innovation from the source of the National Research, Development and Innovation Fund."

References

Böjtösné Varrók, K. (1965): Geological description of the Felsőcsatár talc and serpentine occurrence and examination of the Cr-Ni-Co content. Geological report, Hungarian Geological Institute, p. 81 (in Hungarian)

Butt, C. R. M., Nickel, E. H. (1981): Mineralogy and Geochemistry of the Weathering of the Disseminated Nickel Sulfide Deposit at Mt. Keith, Western Australia. *Economic Geology*, 76, pp. 1736–1751 https://doi.org/10.2113/gsecongeo.76.6.1736

Ditrói-Puskás, Z., Gálné Solymos, K., Kubovics, I., Nagy-Balogh, J., Nagy, B., Hoffmann, L. (1999): Investigation of some pegmatophile and siderophile elements (Sc, Nb, Y, Zr, Ti, V, Cr, Ni, Co) within Hungarian rocks, with special regard to mafic and ultramafic rocks. Geological report, Eötvös Loránd University, Department of Petrology and Geochemistry, Budapest, p. 30 (in Hungarian)

Demény, A., Dunkl, I. (1991): Preliminary zircon fissiontrack results in the Kőszeg Penninic unit, W Hungary. *Acta Mineralogica-Petrographica*, 32, pp. 43–47

Dill, H. G. (2010): The "chessboard" classification scheme of mineral deposits: Mineralogy and geology from aluminum to zirconium. *Earth-Science Review*, 100, pp. 1–420 https://doi.org/10.1016/j.earscirev.2009.10.011

Frank, W., Kralik, M., Scharbert, S., Thöni, M. (1987). Geochronological data from the East Alps. In: Flügel, H. W., Faupl, P. (eds). *Geodynamics of the Eastern Alps,* Deuticke, Wien, pp 272–281

Grguric, B. A. (2002): Hypogene violarite of exsolution origin from Mount Keith, Western Australia: field evidence for a stable pentlandite-violarite tie line. *Mineralogical Magazine*, 66, pp. 313–326 https://doi.org/10.1180/0026461026620032

Grohol, M., Veeh, C. (2023): Study on the critical raw materials for the EU 2023 – Final report. Publications Office of the European Union, 2023. https://data.europa.eu/doi/10.2873/725585

Haas, J., Budai, T., Csontos, L., Fodor, L., Konrád, Gy. (2010): Pre-Cenozoic geological map of Hungary, 1:500 000. Geological Institute Hungary, Budapest.

Kiefer, S., Majzlan, J., Chovan, M., Števko, M. (2017): Mineral compositions and phase relations of the complex sulfarsenides and arsenides from Dobšiná (Western Carpathians, Slovakia). Ore Geology Reviews, 89, 894–908 https://doi.org/10.1016/j.oregeorev.2017.07.026

Koller, F. (1985). Petrologie und Geochemie der Ophiolite des Penninikums and Alpenostrand. *Jahrbuch der Geologischen Bundesanstalt,* 128, pp. 83–150

Majzlan, J., Mikus, T., Kiefer, S., Creaser, R. A. (2022): Rhenium-osmium geochronology of gersdorffite and skutterudite-pararammelsbergite links nickel–cobalt mineralization to the opening of the incipient Meliata Ocean (Western Carpathians, Slovakia). *Mineralium Deposita,* 57, 621–629 https://doi.org/10.1007/s00126-022-01101-7

Pahr, A. (1980): Die Fenster von Rechnitz, Berstein und Moltern. In: Oberhauser, R. (ed). *Der Geologische Aufbau Österreichs*, Springer, Wien, pp 320–326

Ratschbacher, L., Behrmann, I. H., Pahr, A. (1990). Penninic windows at the eastern end of the Alps and their relation to the intra-Carpathian basins. *Tectonophysics*, 172, pp. 91–105, https://doi.org/10.1016/0040-1951(90)90061-C

Tenailleau, C., Pring, A., Etschmann B., Brugger, J., Grguric, B., Putnis, A. (2006): Transformation of pentlandite to violarite under mild hydrothermal conditions. *American Mineralogist*, 91, pp. 706–709 https://doi.org/10.2138/am.2006.2131

Appendix 1a

WDS analytical results and calculated structural formulas of pyrrhotite (normalized to the corresponding number of S atoms).

S wt%	Fe wt%	Co wt%	Ni wt%	Total	Fe_apfu	Co_apfu	Ni_apfu	Cat_sum	Fe_at%	Co_at%	Ni_at%	Formula
39.254	54.971	0.188	5.088	99.501	0.804	0.003	0.071	0.877	91.633	0.297	8.070	Fe0.80 Co0.00 Ni0.07 S
39.686	55.371	0.206	5.353	100.616	0.801	0.003	0.074	0.878	91.282	0.322	8.396	Fe0.80 Co0.00 Ni0.07 S
39.25	55.393	0.209	5.222	100.074	0.810	0.003	0.073	0.886	91.468	0.327	8.204	Fe0.81 Co0.00 Ni0.07 S
39.44	55.831	0.148	4.912	100.331	0.813	0.002	0.068	0.883	92.062	0.231	7.707	Fe0.81 Co0.00 Ni0.07 S
39.726	54.235	0.242	5.693	99.896	0.784	0.003	0.078	0.865	90.571	0.383	9.046	Fe0.78 Co0.00 Ni0.08 S
39.718	54.809	0.202	5.379	100.108	0.792	0.003	0.074	0.869	91.168	0.318	8.513	Fe0.79 Co0.00 Ni0.07 S
39.554	55.087	0.193	5.194	100.028	0.800	0.003	0.072	0.874	91.489	0.304	8.208	Fe0.80 Co0.00 Ni0.07 S
39.795	54.687	0.186	5.506	100.174	0.789	0.003	0.076	0.867	90.990	0.293	8.717	Fe0.79 Co0.00 Ni0.08 S
39.25	55.57	0.198	4.877	99.895	0.813	0.003	0.068	0.884	92.006	0.311	7.683	Fe0.81 Co0.00 Ni0.07 S
39.602	54.541	0.197	5.804	100.144	0.791	0.003	0.080	0.874	90.524	0.310	9.166	Fe0.79 Co0.00 Ni0.08 S
39.776	55.175	0.207	5.72	100.878	0.796	0.003	0.079	0.878	90.728	0.323	8.949	Fe0.80 Co0.00 Ni0.08 S
39.736	55.118	0.209	5.849	100.912	0.796	0.003	0.080	0.880	90.534	0.325	9.141	Fe0.80 Co0.00 Ni0.08 S
39.183	55.243	0.206	5.606	100.238	0.810	0.003	0.078	0.891	90.902	0.321	8.777	Fe0.81 Co0.00 Ni0.08 S
39.463	55.551	0.174	5.451	100.639	0.808	0.002	0.075	0.886	91.213	0.271	8.516	Fe0.81 Co0.00 Ni0.08 S
39.487	56.053	0.202	4.793	100.535	0.815	0.003	0.066	0.884	92.185	0.315	7.500	Fe0.82 Co0.00 Ni0.07 S
39.708	54.94	0.217	5.256	100.121	0.794	0.003	0.072	0.870	91.344	0.342	8.315	Fe0.79 Co0.00 Ni0.07 S
39.728	54.957	0.164	4.52	99.369	0.794	0.002	0.062	0.859	92.500	0.262	7.239	Fe0.79 Co0.00 Ni0.06 S
39.485	54.919	0.173	5.013	99.59	0.799	0.002	0.069	0.870	91.757	0.274	7.969	Fe0.80 Co0.00 Ni0.07 S
39.861	55.431	0.227	5.14	100.659	0.798	0.003	0.070	0.872	91.566	0.355	8.079	Fe0.80 Co0.00 Ni0.07 S
39.888	56.193	0.15	4.003	100.234	0.809	0.002	0.055	0.866	93.431	0.236	6.333	Fe0.81 Co0.00 Ni0.05 S
39.29	55.238	0.195	4.882	99.605	0.807	0.003	0.068	0.878	91.959	0.308	7.733	Fe0.81 Co0.00 Ni0.07 S
39.679	55.415	0.18	4.927	100.201	0.802	0.002	0.068	0.872	91.939	0.283	7.778	Fe0.80 Co0.00 Ni0.07 S
39.572	55.365	0.17	4.923	100.03	0.803	0.002	0.068	0.874	91.953	0.268	7.780	Fe0.80 Co0.00 Ni0.07 S
39.649	54.791	0.21	5.387	100.037	0.793	0.003	0.074	0.871	91.143	0.331	8.526	Fe0.79 Co0.00 Ni0.07 S
39.834	54.89	0.241	5.615	100.58	0.791	0.003	0.077	0.872	90.786	0.378	8.836	Fe0.79 Co0.00 Ni0.08 S
39.563	54.972	0.198	5.679	100.412	0.798	0.003	0.078	0.879	90.768	0.310	8.922	Fe0.80 Co0.00 Ni0.08 S
39.625	54.943	0.262	5.798	100.628	0.796	0.004	0.080	0.880	90.504	0.409	9.087	Fe0.80 Co0.00 Ni0.08 S
39.426	54.518	0.24	5.831	100.015	0.794	0.003	0.081	0.878	90.421	0.377	9.202	Fe0.79 Co0.00 Ni0.08 S

Appendix 1b

WDS analytical results and calculated structural formulas of pyrrhotite (normalized to the corresponding number of S atoms).

S wt%	Fe wt%	Co wt%	Ni wt%	Total	Fe_apfu	Co_apfu	Ni_apfu	Cat_sum	Fe_at%	Co_at%	Ni_at%	Formula
39.497	55.061	0.232	5.667	100.457	0.800	0.003	0.078	0.882	90.751	0.362	8.887	Fe0.80 Co0.00 Ni0.08 S1
39.445	54.943	0.176	5.832	100.396	0.800	0.002	0.081	0.883	90.577	0.275	9.148	Fe0.80 Co0.00 Ni0.08 S1
39.362	55.089	0.226	5.834	100.511	0.804	0.003	0.081	0.888	90.526	0.352	9.122	Fe0.80 Co0.00 Ni0.08 S1
39.607	55.516	0.169	5.471	100.763	0.805	0.002	0.075	0.883	91.187	0.263	8.550	Fe0.80 Co0.00 Ni0.08 S1
39.172	55.171	0.218	5.665	100.226	0.809	0.003	0.079	0.891	90.790	0.340	8.870	Fe0.81 Co0.00 Ni0.08 S1
39.255	54.909	0.196	5.501	99.861	0.803	0.003	0.077	0.882	91.016	0.308	8.676	Fe0.80 Co0.00 Ni0.08 S1
39.445	54.651	0.226	5.723	100.045	0.796	0.003	0.079	0.878	90.616	0.355	9.029	Fe0.80 Co0.00 Ni0.08 S1
39.457	54.861	0.193	5.749	100.26	0.798	0.003	0.080	0.881	90.658	0.302	9.039	Fe0.80 Co0.00 Ni0.08 S1
39.634	54.77	0.239	5.773	100.416	0.793	0.003	0.080	0.876	90.545	0.374	9.081	Fe0.79 Co0.00 Ni0.08 S1
39.718	54.585	0.224	5.956	100.483	0.789	0.003	0.082	0.874	90.276	0.351	9.372	Fe0.79 Co0.00 Ni0.08 S1
39.284	54.504	0.233	5.592	99.613	0.797	0.003	0.078	0.878	90.771	0.368	8.861	Fe0.80 Co0.00 Ni0.08 S1
39.404	54.222	0.232	5.752	99.61	0.790	0.003	0.080	0.873	90.499	0.367	9.134	Fe0.79 Co0.00 Ni0.08 S1
39.351	53.367	0.164	6.607	99.489	0.779	0.002	0.092	0.873	89.229	0.260	10.511	Fe0.78 Co0.00 Ni0.09 S1
39.339	53.33	0.167	6.752	99.588	0.778	0.002	0.094	0.874	89.013	0.264	10.723	Fe0.78 Co0.00 Ni0.09 S1
40.248	55.808	0.138	4.232	100.426	0.796	0.002	0.057	0.855	93.067	0.218	6.715	Fe0.80 Co0.00 Ni0.06 S1
39.697	54.253	0.191	6.452	100.593	0.785	0.003	0.089	0.876	89.566	0.299	10.135	Fe0.78 Co0.00 Ni0.09 S1
39.196	54.28	0.165	6.527	100.168	0.795	0.002	0.091	0.888	89.502	0.258	10.240	Fe0.80 Co0.00 Ni0.09 S1
39.32	53.988	0.185	6.74	100.233	0.788	0.003	0.094	0.885	89.124	0.289	10.587	Fe0.79 Co0.00 Ni0.09 S1
39.446	53.043	0.201	7.794	100.484	0.772	0.003	0.108	0.883	87.459	0.314	12.227	Fe0.77 Co0.00 Ni0.11 S1
39.455	53.213	0.179	7.394	100.241	0.774	0.002	0.102	0.879	88.075	0.281	11.644	Fe0.77 Co0.00 Ni0.10 S1
39.332	53.668	0.162	6.599	99.761	0.783	0.002	0.092	0.877	89.297	0.255	10.447	Fe0.78 Co0.00 Ni0.09 S1
39.286	54.199	0.152	6.425	100.062	0.792	0.002	0.089	0.884	89.650	0.238	10.112	Fe0.79 Co0.00 Ni0.09 S1
39.945	55.208	0.138	5.171	100.462	0.794	0.002	0.071	0.866	91.618	0.217	8.165	Fe0.79 Co0.00 Ni0.07 S1
38.863	54.36	0.167	5.951	99.341	0.803	0.002	0.084	0.889	90.328	0.263	9.409	Fe0.80 Co0.00 Ni0.08 S1
40.621	55.486	0.145	3.212	99.464	0.784	0.002	0.043	0.829	94.558	0.234	5.208	Fe0.78 Co0.00 Ni0.04 S1
40.556	55.509	0.2	3.09	99.355	0.786	0.003	0.042	0.830	94.663	0.323	5.014	Fe0.79 Co0.00 Ni0.04 S1
39.511	54.581	0.175	5.517	99.784	0.793	0.002	0.076	0.872	90.974	0.276	8.749	Fe0.79 Co0.00 Ni0.08 S1
40.196	55.232	0.176	4.308	99.912	0.789	0.002	0.059	0.850	92.830	0.280	6.889	Fe0.79 Co0.00 Ni0.06 S1

Appendix 1c

WDS analytical results and calculated structural formulas of pyrrhotite (normalized to the corresponding number of S atoms).

S wt%	**Fe wt%**	**Co wt%**	**Ni wt%**	**Total**	**Fe_apfu**	**Co_apfu**	**Ni_apfu**	**Cat_sum**	**Fe_at%**	**Co_at%**	**Ni_at%**	**Formula**
39.795	54.966	0.201	5.15	100.112	0.793	0.003	0.071	0.867	91.524	0.317	8.159	Fe0.79 Co0.00 Ni0.07 S1
39.402	54.328	0.182	6.384	100.296	0.792	0.003	0.089	0.883	89.688	0.285	10.028	Fe0.79 Co0.00 Ni0.09 S1
39.581	54.292	0.155	6.487	100.515	0.788	0.002	0.090	0.879	89.574	0.242	10.183	Fe0.79 Co0.00 Ni0.09 S1
39.763	53.547	0.195	6.14	99.645	0.773	0.003	0.084	0.860	89.883	0.310	9.806	Fe0.77 Co0.00 Ni0.08 S1
39.819	54.539	0.197	5.262	99.817	0.786	0.003	0.072	0.861	91.306	0.313	8.382	Fe0.79 Co0.00 Ni0.07 S1
39.37	54.907	0.227	5.561	100.065	0.801	0.003	0.077	0.881	90.886	0.356	8.758	Fe0.80 Co0.00 Ni0.08 S1

Appendix 2a

WDS analytical results and calculated structural formulas of pentlandite (normalized to the corresponding number of S atoms).

S wt%	Fe wt%	Co wt%	Ni wt%	Total	Fe_apfu	Co_apfu	Ni_apfu	Cat_sum	Fe_at%	Co_at%	Ni_at%	Formula
33.034	26.747	1.399	38.224	99.404	3.719	0.184	5.057	8.961	41.506	2.057	56.437	Fe3.72 Co0.18 Ni5.06 S8
32.899	27.85	1.593	38.253	100.595	3.888	0.211	5.082	9.181	42.353	2.296	55.351	Fe3.89 Co0.21 Ni5.08 S8
33.128	27.342	1.339	38.993	100.802	3.791	0.176	5.144	9.111	41.609	1.931	56.460	Fe3.79 Co0.18 Ni5.14 S8
33.219	26.856	1.342	38.84	100.257	3.714	0.176	5.110	8.999	41.264	1.954	56.782	Fe3.71 Co0.18 Ni5.11 S8
33.307	27.044	1.321	38.796	100.468	3.730	0.173	5.091	8.993	41.473	1.920	56.608	Fe3.73 Co0.17 Ni5.09 S8
32.6	27.567	1.241	38.524	99.932	3.884	0.166	5.165	9.215	42.153	1.798	56.049	Fe3.88 Co0.17 Ni5.16 S8
32.64	27.23	1.326	38.607	99.803	3.832	0.177	5.170	9.178	41.751	1.927	56.323	Fe3.83 Co0.18 Ni5.17 S8
32.595	27.18	1.31	38.635	99.72	3.830	0.175	5.180	9.186	41.699	1.904	56.397	Fe3.83 Co0.17 Ni5.18 S8
33.293	26.929	1.299	39.151	100.672	3.715	0.170	5.140	9.025	41.169	1.882	56.949	Fe3.72 Co0.17 Ni5.14 S8
32.915	26.933	1.427	38.978	100.253	3.759	0.189	5.176	9.123	41.200	2.069	56.732	Fe3.76 Co0.19 Ni5.18 S8
33.076	27.236	1.432	39.086	100.83	3.782	0.188	5.165	9.136	41.403	2.063	56.534	Fe3.78 Co0.19 Ni5.16 S8
33.093	27.489	1.387	38.899	100.868	3.816	0.182	5.137	9.135	41.767	1.997	56.236	Fe3.82 Co0.18 Ni5.14 S8
33.301	27.354	1.296	38.836	100.787	3.773	0.169	5.097	9.039	41.740	1.874	56.386	Fe3.77 Co0.17 Ni5.10 S8
32.712	27.664	1.345	38.894	100.615	3.885	0.179	5.196	9.260	41.950	1.933	56.117	Fe3.88 Co0.18 Ni5.20 S8
32.791	27.593	1.391	38.37	100.145	3.865	0.185	5.114	9.164	42.179	2.015	55.806	Fe3.87 Co0.18 Ni5.11 S8
33.193	27.076	1.346	38.928	100.543	3.747	0.177	5.126	9.049	41.407	1.951	56.643	Fe3.75 Co0.18 Ni5.13 S8
32.945	27.707	1.432	38.515	100.599	3.863	0.189	5.109	9.162	42.166	2.065	55.769	Fe3.86 Co0.19 Ni5.11 S8
32.12	27.339	1.342	38.269	99.07	3.910	0.182	5.207	9.299	42.045	1.956	55.999	Fe3.91 Co0.18 Ni5.21 S8
32.31	28.149	1.386	38.025	99.87	4.002	0.187	5.144	9.332	42.882	2.001	55.117	Fe4.00 Co0.19 Ni5.14 S8
32.449	27.625	1.354	38.074	99.502	3.911	0.182	5.128	9.220	42.412	1.970	55.618	Fe3.91 Co0.18 Ni5.13 S8
32.807	27.378	1.311	38.674	100.17	3.833	0.174	5.152	9.159	41.851	1.899	56.250	Fe3.83 Co0.17 Ni5.15 S8
32.235	27.445	1.364	38.37	99.414	3.911	0.184	5.202	9.297	42.064	1.981	55.955	Fe3.91 Co0.18 Ni5.20 S8
33.032	27.742	1.299	38.745	100.818	3.858	0.171	5.126	9.155	42.137	1.870	55.994	Fe3.86 Co0.17 Ni5.13 S8
32.724	27.525	1.355	38.903	100.507	3.864	0.180	5.196	9.240	41.816	1.951	56.233	Fe3.86 Co0.18 Ni5.20 S8
33.129	26.923	1.291	38.878	100.221	3.733	0.170	5.129	9.032	41.332	1.878	56.790	Fe3.73 Co0.17 Ni5.13 S8
33.153	27.366	1.242	39.148	100.909	3.792	0.163	5.161	9.116	41.595	1.789	56.616	Fe3.79 Co0.16 Ni5.16 S8
33.278	27.14	1.31	39.122	100.85	3.746	0.171	5.138	9.056	41.369	1.892	56.739	Fe3.75 Co0.17 Ni5.14 S8
33.181	27.541	1.316	38.55	100.588	3.813	0.173	5.078	9.063	42.068	1.905	56.027	Fe3.81 Co0.17 Ni5.08 S8

Appendix 2b

WDS analytical results and calculated structural formulas of pentlandite (normalized to the corresponding number of S atoms).

S wt%	Fe wt%	C wt%o	Ni wt%	Total	Fe_apfu	Co_apfu	Ni_apfu	Cat_sum	Fe_at%	Co_at%	Ni_at%	Formula
33.228	27.355	0.976	39.3	100.859	3.782	0.128	5.169	9.079	41.653	1.408	56.938	Fe3.78 Co0.13 Ni5.17 S8
33.182	27.195	1.041	39.215	100.633	3.765	0.137	5.165	9.066	41.523	1.506	56.971	Fe3.76 Co0.14 Ni5.17 S8
32.997	27.317	1.092	39.454	100.86	3.803	0.144	5.226	9.173	41.458	1.570	56.972	Fe3.80 Co0.14 Ni5.23 S8
33.374	27.4	0.926	39.206	100.906	3.771	0.121	5.134	9.026	41.780	1.338	56.882	Fe3.77 Co0.12 Ni5.13 S8
32.914	27.841	0.732	39.041	100.528	3.885	0.097	5.184	9.166	42.388	1.056	56.556	Fe3.89 Co0.10 Ni5.18 S8
33.044	27.434	0.877	39.034	100.389	3.814	0.116	5.163	9.092	41.945	1.271	56.785	Fe3.81 Co0.12 Ni5.16 S8
32.858	27.618	0.762	38.951	100.189	3.861	0.101	5.181	9.143	42.229	1.104	56.667	Fe3.86 Co0.10 Ni5.18 S8
32.983	27.7	0.65	39.311	100.644	3.858	0.086	5.209	9.153	42.149	0.937	56.914	Fe3.86 Co0.09 Ni5.21 S8
32.984	27.349	0.773	39.524	100.63	3.809	0.102	5.237	9.148	41.635	1.115	57.250	Fe3.81 Co0.10 Ni5.24 S8
33.277	27.36	0.843	38.99	100.47	3.777	0.110	5.121	9.008	41.927	1.224	56.849	Fe3.78 Co0.11 Ni5.12 S8
32.995	27.367	0.817	38.522	99.701	3.810	0.108	5.103	9.020	42.237	1.195	56.568	Fe3.81 Co0.11 Ni5.10 S8
33.227	27.189	1.051	39.027	100.494	3.759	0.138	5.133	9.030	41.625	1.525	56.850	Fe3.76 Co0.14 Ni5.13 S8
32.698	27.094	0.926	38.458	99.176	3.806	0.123	5.140	9.070	41.965	1.359	56.676	Fe3.81 Co0.12 Ni5.14 S8
33.098	27.497	0.878	39.023	100.496	3.816	0.115	5.153	9.084	42.007	1.271	56.722	Fe3.82 Co0.12 Ni5.15 S8
33.289	27.372	0.841	38.468	99.97	3.777	0.110	5.050	8.937	42.260	1.230	56.510	Fe3.78 Co0.11 Ni5.05 S8
33.886	27.306	0.77	37.27	99.232	3.701	0.099	4.807	8.607	43.003	1.149	55.847	Fe3.70 Co0.10 Ni4.81 S8
33.29	26.463	0.927	38.64	99.32	3.651	0.121	5.073	8.846	41.280	1.370	57.350	Fe3.65 Co0.12 Ni5.07 S8
34.145	26.562	1.023	38.278	100.008	3.573	0.130	4.900	8.603	41.534	1.516	56.950	Fe3.57 Co0.13 Ni4.90 S8
33.13	26.927	0.94	39.456	100.453	3.733	0.124	5.205	9.062	41.198	1.363	57.439	Fe3.73 Co0.12 Ni5.21 S8
33.213	27.138	0.952	39.11	100.413	3.753	0.125	5.147	9.025	41.589	1.383	57.028	Fe3.75 Co0.12 Ni5.15 S8
33.247	27.555	0.988	38.667	100.457	3.807	0.129	5.083	9.019	42.209	1.434	56.357	Fe3.81 Co0.13 Ni5.08 S8
33.069	27.369	1.033	39.277	100.748	3.802	0.136	5.191	9.129	41.645	1.489	56.865	Fe3.80 Co0.14 Ni5.19 S8
32.877	27.493	1.004	38.881	100.255	3.841	0.133	5.169	9.143	42.013	1.454	56.533	Fe3.84 Co0.13 Ni5.17 S8
33.739	27.001	0.815	38.834	100.389	3.676	0.105	5.031	8.812	41.718	1.193	57.089	Fe3.68 Co0.11 Ni5.03 S8
33.453	26.992	1.046	39.101	100.592	3.706	0.136	5.108	8.951	41.407	1.521	57.072	Fe3.71 Co0.14 Ni5.11 S8

Appendix 3a

WDS analytical results and calculated structural formulas of violarite-siegenite group (normalized to the corresponding number of S atoms).

S wt%	Fe wt%	Co wt%	N wt%i	Total	Fe_apfu	Co_apfu	Ni_apfu	Cat_sum	Fe_at%	Co_at%	Ni_at%	Formula
41.632	16.844	0.622	39.498	98.596	0.929	0.033	2.073	3.035	30.617	1.071	68.311	Fe0.93 Co0.03 Ni2.07 S4
41.862	16.46	0.7	39.708	98.73	0.903	0.036	2.073	3.012	29.979	1.208	68.813	Fe0.90 Co0.04 Ni2.07 S4
42.339	17.896	0.529	37.91	98.674	0.971	0.027	1.957	2.955	32.856	0.920	66.224	Fe0.97 Co0.03 Ni1.96 S4
41.969	16.72	0.619	39.331	98.639	0.915	0.032	2.048	2.995	30.550	1.072	68.378	Fe0.91 Co0.03 Ni2.05 S4
41.688	14.199	2.361	40.403	98.651	0.782	0.123	2.118	3.023	25.873	4.077	70.050	Fe0.78 Co0.12 Ni2.12 S4
41.911	13.828	2.387	41.085	99.211	0.758	0.124	2.142	3.024	25.059	4.099	70.842	Fe0.76 Co0.12 Ni2.14 S4
41.835	13.772	2.297	41.059	98.963	0.756	0.119	2.145	3.020	25.033	3.956	71.011	Fe0.76 Co0.12 Ni2.14 S4
41.739	13.821	2.327	40.833	98.72	0.761	0.121	2.138	3.020	25.185	4.018	70.797	Fe0.76 Co0.12 Ni2.14 S4
41.619	13.854	2.481	40.961	98.915	0.765	0.130	2.151	3.045	25.108	4.261	70.632	Fe0.76 Co0.13 Ni2.15 S4
42.099	19.38	2.912	35.033	99.424	1.057	0.151	1.818	3.026	34.936	4.974	60.089	Fe1.06 Co0.15 Ni1.82 S4
42.399	18.797	7.116	31.501	99.813	1.018	0.365	1.624	3.007	33.861	12.147	53.992	Fe1.02 Co0.37 Ni1.62 S4
42.734	18.457	7.47	31.712	100.373	0.992	0.380	1.622	2.994	33.131	12.706	54.162	Fe0.99 Co0.38 Ni1.62 S4
42.289	18.669	7.428	31.456	99.842	1.014	0.382	1.625	3.022	33.555	12.651	53.794	Fe1.01 Co0.38 Ni1.63 S4
42.149	17.12	8.996	31.166	99.431	0.933	0.465	1.616	3.013	30.959	15.416	53.625	Fe0.93 Co0.46 Ni1.62 S4
43.06	17.213	8.69	31.381	100.344	0.918	0.439	1.593	2.950	31.123	14.889	53.987	Fe0.92 Co0.44 Ni1.59 S4
41.988	14.338	2.707	40.054	99.087	0.784	0.140	2.085	3.009	26.063	4.663	69.275	Fe0.78 Co0.14 Ni2.08 S4
42.066	14.138	2.748	39.969	98.921	0.772	0.142	2.076	2.990	25.813	4.754	69.433	Fe0.77 Co0.14 Ni2.08 S4
41.578	16.297	0.889	39.741	98.505	0.900	0.047	2.089	3.035	29.657	1.533	68.810	Fe0.90 Co0.05 Ni2.09 S4
41.77	16.086	0.923	40.107	98.886	0.884	0.048	2.098	3.031	29.183	1.587	69.230	Fe0.88 Co0.05 Ni2.10 S4
42.512	17.566	7.269	32.221	99.568	0.949	0.372	1.656	2.977	31.873	12.498	55.628	Fe0.95 Co0.37 Ni1.66 S4
42.473	20.633	0.744	35.259	99.109	1.116	0.038	1.814	2.968	37.592	1.285	61.123	Fe1.12 Co0.04 Ni1.81 S4
42.365	19.104	3.299	34.599	99.367	1.036	0.169	1.785	2.990	34.640	5.668	59.692	Fe1.04 Co0.17 Ni1.78 S4
42.216	18.897	1.798	35.78	98.691	1.028	0.093	1.852	2.973	34.582	3.118	62.300	Fe1.03 Co0.09 Ni1.85 S4
42.176	19.977	0.692	36.579	99.424	1.088	0.036	1.895	3.019	36.036	1.183	62.782	Fe1.09 Co0.04 Ni1.90 S4
41.79	17.066	0.585	39.786	99.227	0.938	0.030	2.080	3.049	30.763	0.999	68.238	Fe0.94 Co0.03 Ni2.08 S4
42.145	17.329	0.811	38.898	99.183	0.944	0.042	2.017	3.003	31.446	1.395	67.160	Fe0.94 Co0.04 Ni2.02 S4
41.972	22.868	0.472	33.543	98.855	1.251	0.024	1.746	3.022	41.405	0.810	57.786	Fe1.25 Co0.02 Ni1.75 S4
42.04	13.786	2.383	41.605	99.814	0.753	0.123	2.163	3.039	24.781	4.059	71.159	Fe0.75 Co0.12 Ni2.16 S4

Appendix 3b

WDS analytical results and calculated structural formulas of violarite-siegenite group (normalized to the corresponding number of S atoms).

S wt%	Fe wt%	Co wt%	N wt%i	Total	Fe_apfu	Co_apfu	Ni_apfu	Cat_sum	Fe_at%	Co_at%	Ni_at%	Formula
41.782	13.801	2.627	41.347	99.557	0.759	0.137	2.163	3.058	24.808	4.475	70.717	Fe0.76 Co0.14 Ni2.16 S4
42.124	13.663	2.408	41.454	99.649	0.745	0.124	2.151	3.020	24.668	4.120	71.212	Fe0.74 Co0.12 Ni2.15 S4
42.376	24.584	0.683	32.304	99.947	1.332	0.035	1.666	3.033	43.925	1.156	54.918	Fe1.33 Co0.04 Ni1.67 S4
42.315	20.978	0.819	35.419	99.531	1.139	0.042	1.829	3.010	37.829	1.400	60.771	Fe1.14 Co0.04 Ni1.83 S4
42.004	16.672	0.669	38.86	98.205	0.912	0.035	2.022	2.968	30.715	1.168	68.117	Fe0.91 Co0.03 Ni2.02 S4
41.998	16.732	0.733	39.208	98.671	0.915	0.038	2.040	2.993	30.571	1.269	68.160	Fe0.92 Co0.04 Ni2.04 S4
41.951	17.223	0.704	38.952	98.83	0.943	0.037	2.029	3.008	31.342	1.214	67.444	Fe0.94 Co0.04 Ni2.03 S4
41.937	16.909	0.72	39.08	98.646	0.926	0.037	2.036	3.000	30.870	1.246	67.884	Fe0.93 Co0.04 Ni2.04 S4
41.735	17.389	0.731	39.086	98.941	0.957	0.038	2.047	3.042	31.461	1.253	67.285	Fe0.96 Co0.04 Ni2.05 S4
41.782	15.768	2.847	38.641	99.038	0.867	0.148	2.021	3.036	28.549	4.885	66.567	Fe0.87 Co0.15 Ni2.02 S4
42.341	15.504	13.215	29.7	100.76	0.841	0.679	1.533	3.053	27.545	22.248	50.206	Fe0.84 Co0.68 Ni1.53 S4
42.231	19.361	11.97	26.386	99.948	1.053	0.617	1.365	3.035	34.691	20.324	44.985	Fe1.05 Co0.62 Ni1.37 S4
42.156	14.892	13.661	29.194	99.903	0.811	0.705	1.513	3.030	26.777	23.277	49.946	Fe0.81 Co0.71 Ni1.51 S4
42.238	14.881	13.445	29.327	99.891	0.809	0.693	1.517	3.019	26.800	22.945	50.254	Fe0.81 Co0.69 Ni1.52 S4
42.18	15.421	13.099	29.45	100.15	0.840	0.676	1.526	3.041	27.609	22.223	50.168	Fe0.84 Co0.68 Ni1.53 S4
42.298	15.703	13.107	29.199	100.307	0.853	0.674	1.509	3.036	28.089	22.216	49.695	Fe0.85 Co0.67 Ni1.51 S4
42.131	15.302	13.415	29.493	100.341	0.834	0.693	1.530	3.057	27.288	22.669	50.043	Fe0.83 Co0.69 Ni1.53 S4
41.838	14.913	13.972	29.235	99.958	0.819	0.727	1.527	3.072	26.645	23.656	49.699	Fe0.82 Co0.73 Ni1.53 S4
41.772	15.587	13.282	29.218	99.859	0.857	0.692	1.529	3.078	27.847	22.486	49.667	Fe0.86 Co0.69 Ni1.53 S4
42.724	14.962	13.003	29.78	100.469	0.804	0.662	1.523	2.990	26.901	22.154	50.945	Fe0.80 Co0.66 Ni1.52 S4
42.485	15.091	12.989	30.013	100.578	0.816	0.665	1.544	3.025	26.969	21.997	51.034	Fe0.82 Co0.67 Ni1.54 S4
42.737	15.593	12.327	30.151	100.808	0.838	0.628	1.542	3.007	27.864	20.873	51.263	Fe0.84 Co0.63 Ni1.54 S4
42.581	15.379	12.175	30.437	100.572	0.830	0.622	1.562	3.014	27.523	20.648	51.829	Fe0.83 Co0.62 Ni1.56 S4
42.422	15.419	11.782	30.35	99.973	0.835	0.604	1.563	3.003	27.802	20.131	52.068	Fe0.83 Co0.60 Ni1.56 S4